Comparison of Flow and Batch Polymerization Processes for Production of Vinyl Ether Terpolymers for Use in the Delivery of siRNA

Jason L. Nyrop,[1] Arash Soheili,[2] Rong Xiang,[3] Fanyu Meng,[3] Jacob H. Waldman,[2] Xiujuan Jia,[3] Rubina Giarre Parmar,[4] Benjamin W. Thuronyi,[4] J. Michael Williams,[4] Lisa DiMichele,[2] Michel Journet,[2] Bonnie J. Howell,[5] Bing Mao,[3] Ian W. Davies,[2] Steven L. Colletti,[4] Laura Sepp-Lorenzino,[5] Erin N. Guidry[2]

[1]Department of Chemical Engineering, Merck & Co., Inc., Rahway, New Jersey 07065
[2]Department of Process Chemistry, Merck & Co., Inc., Rahway, New Jersey 07065
[3]Department of Analytical Chemistry, Merck & Co., Inc., Rahway, New Jersey 07065
[4]Department of Medicinal Chemistry, Merck & Co., Inc., West Point, Pennsylvania 19486
[5]Department of RNA Biology, Merck & Co., Inc., West Point, Pennsylvania 19486
Correspondence to: E. N. Guidry (E-mail: erin_guidry@merck.com)

ABSTRACT: Synthetic polymers represent a modifiable class of materials that can serve as adjuvants to address challenges in numerous biomedical and medicinal chemistry applications including the delivery of siRNA. Polymer-based therapeutics offer unique challenges in both synthesis and characterization as compared to small molecule therapeutics. The ability to control the structure of the polymer is critical in creating a therapeutic. Reported herein, are batch and flow polymerization processes to produce amphiphilic terpolymers through a Lewis acid BF_3OEt_2-catalyzed polymerization. These processes focus on controlling reaction variables, which affect polymer struc-ture in this rapid, exothermic, nonliving cationic polymerization. In addition to analytical characterization of the polymers, the *in vivo* activity of the polymer-siRNA conjugates is also highlighted—demonstrating that the method of synthesis does affect the *in vivo* activity of the resulting polymer conjugate. © 2014 Wiley Periodicals, Inc. J. Polym. Sci., Part A: Polym. Chem. **2014**, *52*, 1119–1129

KEYWORDS: amphiphiles; biological applications of polymers; cationic polymerization; copolymerization; drug delivery systems; poly(vinyl ethers)

INTRODUCTION Polymer-based delivery has received increasing attention in the field of medicinal chemistry and biotechnology including the delivery of short interfering RNA (siRNA).[1–8] The ability to control the character of the polymer structure in terms of size and monomer incorporation provides a unique opportunity for chemists to optimize the delivery vehicle in concert with its payload.[9–32] Therefore, careful control of the polymer synthesis is required and may provide an opportunity to create a differentiated therapeutic. In a recent report by Rozema et al., a poly(vinyl ether) (PVE)-based cationic–amphiphilic polymer–siRNA conjugate was reported to effect liver-targeted delivery of siRNA and produce mRNA knockdown (KD) in a rodent model.[9] The cationic–amphiphilic PVE copolymer used to prepare the polymer–siRNA conjugate was prepared through a nonliving BF_3OEt_2-catalyzed polymerization. While the molecular weight, polydispersity, and overall monomer content can be measured for the terpolymer, little direct structural information regarding the nature of monomer incorporation or tacticity could readily be obtained by available analytical methods. For this reason, the process by which the polymer is prepared defines the structure of the polymer produced. As such, it is critical to develop reproducible and scaleable polymerization processes that control variables, such as temperature and mixing, which affect polymer molecular weight, tacticity, and monomer incorporation. In this article, we describe two methods, a modified batch process and flow polymerization process, that control these variables, enabling reproducible polymer synthesis. In addition to analytical characterization of the polymers produced by these two methods, the *in vivo* activity of their corresponding polymer conjugates will also be reported; highlighting that *in vivo* activity is affected by the polymerization method.

EXPERIMENTAL

Materials

Unless otherwise noted, all chemicals were obtained from the Aldrich Chemical Company. Carboxydimethylmaleic anhydride poly(ethylene glycol) (CDM-PEG; $M_w = 680$ g/mol)

Additional Supporting Information may be found in the online version of this article.

and carboxydimethylmaleic anhydride N-acetylgalactosamine (CDM-NAG) were synthesized according to the literature procedure.[9] The siRNA targeting ApolipoproteinB using the Zimmerman pattern[38] was used.

5′-amil-GGAAUC<u>UU</u>A<u>U</u>A<u>UUU</u>GA<u>UCC</u>AsA-3′

3′-Us<u>C</u>s<u>C</u>C<u>U</u>UAGAA<u>U</u>A<u>U</u>AAA<u>C</u>UAGG<u>UU</u>-5′

amil = amino linker; <u>UC</u> = 2′-methoxy (OMe); AUG= ribose; s= phosphorothioate linkage.

The siRNA with an irrelevant sequence (Low Hex 9) was used as a control.

5′-amil-iB-**CU***AG***CU***GGA***CACG***UC***GA***U**A*T*s*T*-iB-3′

3′-Us<u>U</u>GA<u>U</u>**C**GA**CCU**G<u>U</u>G**C**AG**C**UAU-5′

amil = amino linker; iB = Inverted deoxy abasic; **CU** = 2′-fluoro (F); *AGT* = 2′-deoxy; <u>UGA</u> = 2′-methoxy (OMe); AU= ribose; s= phosphorothioate linkage.

Synthesis of N-(2-Vinyloxy-ethyl)phthalimide Monomer

Potassium phthalimide (1400 g, 1 equiv.) was suspended in DMF (5 L). The resulting mixture was heated to 93 °C, and then tetrabutylammonium bromide (48.67 g, 0.02 equiv.) was added. The mixture was stirred for 0.5 h. The reaction mixture was cooled to 60–70 °C, and 2-chloroethyl vinyl ether (1006.8 g, 1.25 equiv.) was added dropwise over 30 min. The reaction mixture was heated to 90–100 °C for 1 h. The mixture was cooled to 50–60 °C, and then water (2.0 L) was added dropwise over 1 h. The mixture was cooled to 20–30 °C and aged for 30 min. The mixture was filtered through a Celite pad, the solid was washed with water (2 × 1 L). The above solids were dissolved in CH_2Cl_2 (7 L). The solution was concentrated to about 3–4 L, until solids appeared. Cyclohexane (5 L) was added dropwise, and the mixture was further concentrated to 2–3 L at 45–50 °C. The mixture was cooled to 10–20 °C and stirred for 30 min. The mixture was filtered and the cake was washed with cyclohexane (2–3 L). The wet cake was dried under vacuum at 40 °C for 12 h. The desired product (PiEVE, 1.37 kg) was obtained with 99.87% LCAP (0.13% of alcohol impurity) and 99.6% LCWP in 83.2% corrected yield.

^{1}H NMR ($CDCl_3$, 500 MHz): δ 7.86 (dd, 2H, J = 5.3, 3.0 Hz), 7.72 (dd, 2H, J = 5.4, 3.0 Hz), 6.42 (dd, 1H, J = 14.4, 6.8 Hz), 4.20 (d, 1H, J = 14.4, 2.2 Hz), 4.01 (m, 3H), 3.94 (m, 2H). GC was used to measure residual solvent. The following solvents were present in the following quantities: MeOH <100 ppm, DCM 540 ppm, cyclohexane 320 ppm, 2-chloroethyl vinyl ether <100 ppm, and DMF <100 ppm.

Purification of Butyl Vinyl Ether

n-Butyl vinyl ether (n-BVE) was purchased from Aldrich and contained a stabilizer, 0.01% KOH. The peroxide content of BVE was measured before distillation and was measured to be <1 ppm (below limit of detection) using QuantofixPeroxide 100 test strips. An NH_3-rinsed and oven-dried 2 L, three-neck round-bottomed flask with magnetic stir bar and internal thermocouple probe was set up in a heating mantle and was fitted with a 14/20 Vigreux column (15 cm), distillation head with water-cooled condenser, and collection flask in a cold bath and purged with nitrogen for 15 min. The flask was charged with BVE (1.50 L). The nitrogen line was moved from the distillation pot to the collection flask and the pot was heated to 100 °C (internal temperature of 95 °C) to begin distillation into a dry ice/acetone-cooled collection flask. Fractions (150–200 mL, colorless liquid) were collected until <200 mL remained in the pot. Fractions were checked by ^{1}H NMR for purity ($CDCl_3$). Fractions containing large amounts of water, noted by ice crystals in the collection flask, were discarded.

Purification of Octadecyl Vinyl Ether

Octadecyl vinyl ether (ODVE) was purchased from TCI. The distillation apparatus was set up behind a blast shield. An ammonia-rinsed 500-mL, three-neck round-bottomed flask with large magnetic stir bar and internal thermocouple probe was fitted with a 24/40 Vigreux column (30 cm) with distillation head and air-cooled condenser. The flask was set up in a heating mantle. The Coolant (water or air) in condenser should be warmed to room temperature to prevent clogging of distillation equipment. ODVE (500 mL) was first warmed to 45 °C to liquefy, and this was then charged to the flask. The system was evacuated and purged with nitrogen three times to remove air (oxygen). The flask was evacuated (1 mmHg) and heated to 190–195 °C (internal temperature of 185–190 °C). The flask was wrapped with glass wool with aluminum foil outside that to contain heat but the Vigreux column was left open to the air to create a better temperature gradient. Fractions were collected until <100 mL remained in the pot. Each fraction was warmed to 40 °C to melt before sampling for GC analysis. By GC, the ratio of C18-vinyl ether:C16-vinyl ether >98:2 was achieved after distillation.

Synthesis of Polymer 1
Synthesis of 18 kDa 15:4:1 [PiEVE:BVE:ODVE] by Flow Polymerization

The monomer solution was prepared by dissolving ODVE (0.734 g, 2.5 mmol, 1 equiv.), n-BVE (0.99 g, 9.9 mmol, 4 equiv.), and N-(2-vinyloxy-ethyl)phthalimide (PiEVE; 8.03 g, 37 mmol, 15 equiv.) dichloromethane (150 mL) with a water content of 100 ppm. The catalyst solution was prepared by dissolving boron trifluoroetherate (0.107 g, 1.5 mol % vs. monomers) dichloromethane (5.23 mL) with a water content of 100 ppm. The quench solution was prepared by dissolving 2M ammonia in methanol (1.5 mL, 4 equiv. versus boron trifluoride diethyl etherate) dichloromethane (103 mL). Stream 1 is pumped at 1.429 mL/min through 1/16″ PTFE and 316 stainless steel tubing introduced to a controlled bath set at −30 °C. Stream 2 is pumped at 0.0714 mL/min through 1/16″ PTFE and 316 stainless steel tubing introduced to the controlled bath. Streams 1 and 2 mix in a 1-mm ID 316 stainless steel tee before entering a 30 mL coil of 1/8″ 304 stainless steel tubing. Stream 3 is pumped at 1.429 mL/min

through 1/16″ PTFE and 316 stainless steel tubing introduced to the controlled bath before mixing with the resulting stream from the 30 mL coil (mixture of Streams 1 and 2) in a 1-mm ID 316 stainless steel tee. The resulting stream exits the controlled bath to a collection vessel. The collected polymer was isolated by removal of dichloromethane under reduced pressure to afford the product polymer **1** with a molecular weight of M_w = 18.1 kDa and polydispersity index of 1.7.

^{1}H NMR (500 mHz, CDCl$_3$) = δ 7.8-7.6 (om), 3.9–3.0 (om), 1.9–1.1 (om), 1.0–0.7 (om).

Synthesis of Polymer 2
Synthesis of 18 kDa 15:4:1 [PiEVE:BVE:ODVE] by Batch Polymerization
In a dry, three-neck flask fitted with an overhead stirrer, nitrogen inlet, and temperature probe was charged dichloromethane (112 mL, <10 ppm H$_2$O). The flask was cooled to −40 °C (cryocool bath) then charged BF$_3$-Et$_2$O (1.19 mL, 9.44 mmol). In a separate round bottom flask dissolved *n*-BVE (48.9 mL, 378 mmol), ODVE (28 g, 94.0 mmol), and PiEVE (308 g, 1416 mmol) in dichloromethane (2100 mL, <10 ppm H$_2$O). The solution of vinyl ether monomers was then charged to the reaction vessel over 1 h at a constant rate using a Knauer pump. The solution was then let stir for an additional 1 h and then quenched with NH$_3$ in MeOH (2.0M, 47 mL) and removed from the cooling bath. Once at room temperature, the reaction mixture was transferred to a recovery flask concentrated *in vacuo* to yield product polymer **2** (376 g, 598 mmol, 101% yield) as a foamy white solid with a molecular weight of M_w = 18.3 kDa and polydispersity index of 1.8.

^{1}H NMR (500 mHz, CDCl$_3$) = δ 7.8−7.6 (om), 3.9−3.0 (om), 1.9−1.1 (om), 1.0−0.7 (om).

Synthesis of Polymer 3
Synthesis of 27.1 kDa 15:4:1 [PiEVE:BVE:ODVE] by Flow Polymerization
The monomer solution was prepared by dissolving ODVE (6.31 g, 21.27 mmol, 1 equiv.), *n*-BVE (8.52 mL, 85.07 mmol, 4 equiv.), and PiEVE (69.30 g, 319.02 mmol, 15 equiv.) in dichloromethane (900 mL) with a water content of 50 ppm. The catalyst solution was prepared by dissolving boron trifluoroetherate (0.92 g, 6.48 mmol, 1.5 mol % vs. monomers) and dichloromethane (45 mL) with a water content of 50 ppm. The quench solution was prepared by combining 2M ammonia in methanol (12.96 mL, 25.91 mmol, 4 equiv. vs. boron trifluoride diethyl etherate) was dissolved in dichloromethane (887 mL). To generate polymer, Stream 1 (monomer solution) was pumped at 1.429 mL/min through 1/16″ PTFE and 316 stainless steel tubing introduced into the controlled temperature bath set at −30 °C. Stream 2 (catalyst solution) was pumped at 0.0714 mL/min through 1/16″ PTFE and 316 stainless steel tubing introduced into the controlled temperature bath. Streams 1 and 2 were mixed in a 1-mm ID 316 stainless steel tee before entering a 30 mL coil of 1/8″ 304 stainless steel tubing. Stream 3 (quench solution) was pumped at 1.429 mL/min through 1/16″ PTFE and 316 stainless steel tubing introduced to the controlled

bath before mixing with the resulting stream from the 30 mL coil (mixture of Streams 1 and 2) in a 1-mm ID 316 stainless steel tee. The resulting stream exited the controlled bath into a collection vessel. The collected polymer was isolated by removal of solvent under reduced pressure to afford the product polymer **3a** with a molecular weight of M_w = 27.1 kDa and polydispersity index of 2.2.

^{1}H NMR (500 mHz, CDCl$_3$) = δ 7.8–7.6 (om), 3.9–3.0 (om), 1.9–1.1 (om), 1.0–0.7 (om). The same procedure was utilized to synthesize two subsequent batches of polymer 3.

Polymer 3b
M_w = 29.4 kDa and polydispersity index of 2.0. ^{1}H NMR (500 mHz, CDCl$_3$) = δ 7.8–7.6 (om), 3.9–3.0 (om), 1.9–1.1 (om), 1.0–0.7 (om).

Polymer 3c
M_w = 28.0 kDa and polydispersity index of 2.8. ^{1}H NMR (500 mHz, CDCl$_3$) = δ 7.8–7.6 (om), 3.9–3.0 (om), 1.9–1.1 (om), 1.0–0.7 (om).

Polymer Deprotection and Purification
All polymers were deprotected and purified by the same general procedure. The deprotection of polymer **2** is given as an example. In a three-neck flask fitted with an overhead stirrer, reflux condenser, and nitrogen inlet was slurried polymer **2** (50.0 g, 79 mmol) in 2-propanol (1000 mL). Hydrazine (25% wt in H$_2$O) (499 mL, 3889 mmol) was charged to the reaction vessel, and the reaction vessel was heated (65 °C). After 16 h, the reaction mixture was cooled to room temperature. A constant volume distillation was performed to remove 2-propanol while adding 0.1M NaOH to maintain a volume of 1500 mL of total reaction volume. The distillation was continued until the amount of 2-propanol remaining in the reaction mixture was below 1% of the total volume as monitored by GC. The aqueous polymer solution was then subjected to tangential flow filtration (TFF) purification (PALL centremate membrane, 1K M_w cutoff, OS001C12) with NaOH (0.25 N) until the high-performance liquid chromatograph (HPLC) of the retentate polymer solution indicated complete removal of phthalhydrazide. The TFF process was continued using water until the pH of waste stream (permeate) became neutral (pH 7–8). The aqueous solution was then freeze-dried to obtain the product polymer **2**-deprotected (20.3 g) as a sticky oil. The water content of the isolated polymer was determined by thermogravimetric analysis. The sodium content of the isolated polymer was determined by inductively coupled plasma (ICP)-MS. The weight percent of the isolated polymer was determined by subtracting the weight of water and sodium hydroxide in the polymer solid from the total weight of polymer solid.

^{1}H NMR (500 mHz, D$_2$O) = δ 3.8–3.0 (om), 2.8–2.6 (om), 2.0–1.0 br, 0.9–0.7 (om).

Proton NMR
The ^{1}H spectra were recorded on a Bruker AV or DPX series NMR spectrometer at a frequency of 400 MHz or 500 MHz

as noted and internally referenced to residual HOD at 4.80 ppm, CHD_2Cl_2 at 5.32 ppm or $CHCl_3$ at 7.27 ppm. Data for ^1H NMR are reported as follows: chemical shift (δ), multiplicity (s = singlet, d = doublet, t = triplet, q = quartet, m = multiplet, o=overlapped, br = broad multiplet) integration, and coupling constant (Hz). ^1H NMR spectra were in full accordance with the expected structures.

Molecular Weight Determination Using Size Exclusion Chromatography

Polymer molecular weight determination for protected polymers was performed on an Agilent 1100 HPLC coupled with a Wyatt miniDAWN™ TREOS [three-angle multiangle light scattering (MALS) system] and a Wyatt Optilab® T-rEX (refractive index detector). Chromatography was performed using two size exclusion chromatographic columns in tandem, Waters Styragel HR3 Column, 5 μm, 7.8 × 300 mm (THF) and Waters Styragel HR4E Column, 5 μm, 7.8 × 300 mm (THF) with 100% THF as mobile phase at a flow rate of 1.0 mL/min. The temperature of the column was set at 25 °C, and the UV detection wavelength was 260 nm. The polymer sample was dissolved in THF at 1–10 mg/mL and 0.5 mg material was injected. Instrument normalization and calibration was performed using 2–40K polystyrene standards with a PDI of less than 1.1 (Polymer Laboratories). No calibration standards were used in determination of molecular weights or polydispersities. The dn/dc values were obtained for each injection assuming 100% mass elution from the columns. These values were also independently verified by measuring the dn/dc independently using a Wyatt Optilab® T-rEX refractometer. The data was collected and processed using Wyatt Astra software. Deprotected polymer molecular weight was not measured directly. Deprotected molecular weight values were calculated by adjusting the corresponding protected molecular weight based on the mass loss due to removal of the protecting group.

SATA Modification of Amino Zimmerman ApoB Oligonucleotide

Amino Zimmerman ApoB Oligonucleotide

Amino zimmerman ApoB oligonucleotide (1 g, 0.0714 mmol) was dissolved in 0.1 M sodium bicarbonate buffer (20 mL, 50 mg/mL) in a vial with magnetic stir bar and cooled to 0–5 °C in an ice water bath. In a separate vial SATA (83 mg, 0.357 mmol, 5 equiv.; Thermo Scientific part 26102) was dissolved in 0.78 mL DMSO. The SATA solution was added over 1 min and the clear, colorless reaction mixture stirred at 0–5 °C for 2 h. After 2 h, the reaction mixture was sampled and analyzed by HPLC for consumption of the starting oligonucleotide. The reaction mixture was purified by dialysis Millipore Amicon Ultra-15 Centrifugal Filter Unit with Ultracel-3 Membrane, UFC900324 using endonuclease free water until HPLC indicated the removal of N-hydroxysuccinimide, and *N*-succinimidyl-*S*-acetylthioacetate. The recovered solution was lyophilized to afford the product SATA-ZimmApoB as a white fluffy solid. Sata Modified LH9 was prepared by an identical procedure.

Polymer Conjugate Synthesis

All polymer conjugates were prepared using the same general procedure. Synthesis of polymer conjugate **2a′** is pro-

vided as an example. Polymer **2**-deprotected (1.2 g) was placed in a 40 mL vial and was dissolved in 100 mM sterile TRIS buffer at pH 9 (120 mL, 10 mg/mL) and added to a 1-L sterile plastic bottle. To this solution was added SMPT (Thermo Scientific) as 1 mg/mL solution in DMSO (18 mg, 1800 μL) corresponding to 1.5 wt % with respect to the polymer weight. The solution was stirred for 1 h at rt to generate activated polymer. The activated polymer solution was further diluted using 100 mM sterile TRIS buffer at pH 9 (496 mL), followed by the addition of sata-modified siRNA sata-ZimmApoB as a solution in water (250 mg, 32.4 mg/mL, 7716 μL). This solution was aged for 4 h at room temperature to generate the siRNA-polymer conjugate. In a separate 1-L sterile plastic bottle, solid CDM-NAG (5.5 g) and CDM-PEG (2.85 g) was added. The siRNA-polymer conjugate solution was transferred by pouring into the plastic bottle containing the CDM-NAG and CDM-PEG solids. The mixture was stirred for 2 min to dissolve all solids and then transferred by pouring into the original plastic bottle, which contained the siRNA-polymer conjugate. The reaction was stirred for 1 h to generate the product masked siRNA-polymer conjugate. The pH of the final solution was monitored to ensure the pH was 8–9 throughout the conjugation process. Purification of the masked polyconjugate was performed using a TFF purification process. The amount of siRNA covalently attached to PVE polymers (conjugation efficiency) was determined using strong anion exchange chromatography (SAX). The conjugation efficiency of the product **2a′** was measured as 89% by SAX (Table 3). The percentage of amines in a PVE polymer that are covalently modified with disubstituted maleimides CDM-NAG and CDM-PEG (molar basis) was determined by HPLC (masking efficiency). The masking efficiency of the product **2a′** was measured as 50% (Table 3). The RNA concentration in the product **2a′** was measured using ICP, and this concentration was used in determining dilutions/dosage volumes for *in vivo* studies.

Masked Polymer Conjugate Purification Process

A TFF process was used to purify masked polymer conjugate formulations (i.e., **2a′**) of unincorporated components and to exchange buffer to a pharmaceutically acceptable formulation vehicle. The TFF filter material was made of either modified polyethersulfone (PES) or regenerated cellulose. The selection of molecular weight cutoff for these membranes was done with efficiency of purification and retention of polymer conjugate in mind. The processing parameters, including but not limited to feed pressure, retentate pressure, crossflow rate, and filtrate flux were set to allow reproducibility from batch to batch and linear scaling of the process. Using the diafiltration mode of TFF, the reaction impurities were filtered out into the permeate, while the retained polymer conjugate underwent a buffer exchange. After TFF, the final product was concentrated to 0.4–2.0 mg/mL of siRNA and sterile filtered using a 0.2-μm PES syringe filter and stored at −20 °C until use.

Conjugation Efficiency (siRNA-Polymer Conjugation)

SAX HPLC is used to determine the conjugation efficiency by analyzing the final masked polyconjugate with and without

dithiothreitol (DTT) treatment. Polymer conjugate solutions were injected neat and as as a 1:1 mixture with 1.0M DTT onto a Proteomix SAX-NP3 Column (Sepax Technologies, 3.0 μM, 100×4.6 mm^2), with Mobile Phase A = 100 mM TRIS (pH 8.0), 10% ACN, and Mobile Phase B = 100 mM TRIS (pH 8.0), 10% ACN, 2M LiCl with a gradient of 0 to 100% B. Free RNA duplex as well as free RNA duplex-dimer was visualized using SAX chromatography. Total RNA (both free and bound) was determined by using ICP spectroscopy. As the RNA is the only phosphorus containing species in the formulations, determining the total phosphorus content can be used to directly determine the total RNA concentration. Once the free RNA (duplex and duplex-dimer) and total RNA is determined, the amount of RNA conjugated to the polymer can be calculated (i.e., conjugation efficiency). Total RNA (bound and unbound RNA and RNA dimer) can also be determined and visualized by pre-treatment of the polyconjugate with DTT before SAX chromatography. Conjugation efficiencies are reported for all PVE polymer conjugates in the text of the article.

Masking Efficiency

Total concentrations of CDM-NAG and CDM-PEG were determined using reverse-phase HPLC (UV at a wavelength of 260 nm) with mobile phases of 0.1% TFA in water and 0.1% TFA in 70/30 methanol:acetonitrile. Rapid demasking of the polymer after injection onto the column allows quantitation of CDMs with the polymer removed using a C18 guard column to prevent chromatographic interference. Free (i.e., unbound) CDM-NAG and CDM-PEG is analyzed by first filtering through a 10 K centrifuge filter followed by analysis of the permeate using the same reverse-phase HPLC method. Masking efficiency can be calculated by first calculating the bound RNA, CDM-NAG, and CDM-PEG. The polymer molecular weight in combination with the total amines available for conjugation is then used with the bound ligands to calculate masking efficiency. Masking efficiencies are reported for all PVE polymer conjugates in Table 3.

In Vivo Evaluation of Efficacy in Mice

CD1 mice were tail vein injected with the siRNA containing polymer conjugates at a specified dose (mg/kg) in a volume of 0.2 mL, 100 mM TRIS/9% glucose, pH9, vehicle. Forty-eight hours post dose, mice were sacrificed and liver tissue samples were immediately preserved in RNALater (Ambion). Preserved liver tissue was homogenized and total RNA isolated using a Qiagen bead mill and the Qiagen miRNA-Easy RNA isolation kit following the manufacturer's instructions. Liver ApoB mRNA levels were determined by quantitative RT-PCR. Message was amplified from purified RNA utilizing primers against the mouse ApoB mRNA (Applied Biosystems Cat. No. Mm01545156_m1). The PCR reaction was run on an ABI 7500 instrument with a 96-well Fast Block. The ApoB mRNA level is normalized to the housekeeping PPIB mRNA and GAPDH. PPIB and GAPDH mRNA levels were determined by RT-PCR using a commercial probe set (Applied Biosytems Cat. No. Mm00478295_m1 and Mm4352339E_m1). Results

are expressed as a ratio of ApoB mRNA/PPIB/GAPDH mRNA. All mRNA data are expressed relative to the vehicle control.

RESULTS AND DISCUSSION

BF$_3$OEt$_2$ Lewis acid-catalyzed cationic polymerizations of vinyl ether monomers are known to be quite rapid and exothermic due to the conversion of pi-bonds to sigma-bonds during chain propagation[33,34] making these types of polymerizations a challenge to control through a typical batch polymerization due to poor heat dissipation and mass transport.[34–36] From the literature, it is evident that a number of variables, such as (1) monomer solubility, (2) temperature, (3) monomer concentration, (4) water content/monomer purity, and (5) method of mixing/monomer addition, could affect polymer structure and molecular weight in a nonliving BF$_3$OEt$_2$-catalyzed cationic copolymerization (Fig. 1).[33,34] While concentration, monomer solubility, water content, and monomer purity could readily be addressed in a traditional batch process, controlling temperature, and mixing is more difficult given the rapid reaction kinetics. Two processes were developed, a flow chemistry process and a modified batch chemistry process, to address the poor heat dissipation and mass transport issues associated with a traditional batch process and allow for improved control of the resulting polymer structure.

Flow Polymerization Process

BF$_3$OEt$_2$ Lewis acid-catalyzed cationic polymerizations of vinyl ether monomers are known to be quite rapid and exothermic, and while this can make these types of polymerizations a challenge to control through a typical batch polymerization, these reaction characteristics made this polymerization an ideal candidate for a flow microreactor-based approach.[35–37] The small dimensions of flow microreactors enable extremely rapid mixing due to short diffusion pathways and the large surface-area-to-volume ratios allow for efficient heat exchange properties.

The first step in optimization of the flow process was to design a flow reactor that would control the reaction parameters, such as temperature and mixing, that had been identified as potentially affecting polymer structure and molecular weight. In the design, a reaction stream containing a mixture of the desired monomers was combined with the BF$_3$OEt$_2$ catalyst solution by flowing these solutions into a mixing tee, which results in very rapid and efficient mixing and rapid heat dissipation. The tubing containing the monomer solution and catalyst solutions were immersed in a temperature-controlled bath, which allowed for thermal equilibration of the catalyst and monomer streams before their combination in the mixing tee. After the monomer stream and catalyst stream were combined in the first mixing tee, the resulting crude polymerization stream was combined in a mixing tee with a quench stream containing a solution of ammonia in methanol. Again, the quench stream was immersed in a temperature-controlled bath which allowed for thermal equilibration of the quench solution before combining with the polymerization stream (Fig. 1). The minimum residence

FIGURE 1 (A) Synthesis of Lewis acid-catalyzed amphiphilic terpolymer. (B) Graphical representation of flow reactor used to produce polymers **1** and **3**. (C) Graphical representation of batch polymerization reaction apparatus used to produce polymer **2**.

time necessary for complete monomer consumption was controlled by the length of the tubing between the first and second mixing tee (i.e., the length of tubing between initial mixing of the monomer and catalyst and the quench). Residence time was optimized experimentally by varying the tubing length and monitoring for the presence of residual monomer in the quenched reaction stream. Solvent water content and temperature affect the polymer molecular weight produced using the flow reactor. As can be seen in Table 1, increasing water content decreases polymer molecular weight, and decreasing the reaction temperature increases polymer molecular weight.

Modified Batch Polymerization: An Inverse Monomer Addition Process

In the traditional batch process used by Rozema et al.,[9] BF_3OEt_2 was added rapidly to a cooled solution of monomers. While this approach does afford polymer, the reaction is quite rapid and exothermic and reaction times of less than 1 minute for complete monomer consumption were observed. In order to overcome the poor heat dissipation and mixing observed in a traditional round bottom reaction vessel, a batch process was developed in which a solution of

monomers was added very slowly to a solution of BF_3OEt_2 at a rate such that mixing and reaction exotherm could be adequately controlled (34.3 mmol/min, Fig. 1). No polymerization was observed at temperatures below $-60\ °C$ and so $-40\ °C$ was selected as the lowest temperature for polymerization evaluation. While it was not possible to reach molecular weights as high as in the flow polymerization process (max $M_w = 18$ kDa vs. > 30 kDa), molecular weights could still be controlled by solvent water content and reaction temperature (Table 2).

In Vivo Comparison of Flow versus Modified Batch Processes

In order to examine the biological properties of PVEs produced using the modified batch and flow processes, polymer-siRNA conjugates made from both processes were prepared. The polymer conjugates, based on those reported by Rozema consist of a polymer conjugated to siRNA through a cytosolically labile disulfide bond. N-Acetylgalactosamine (NAG), a hepatocyte-specific targeting ligand for the asialo-gylcoprotein receptor, and PEG were conjugated to primary amines of the polymer through an acid labile CDM linkage (Fig. 2).[9] In order to eliminate molecular weight as a

TABLE 1 Demonstration of the Relationship of Water Content and Temperature to Polymer Molecular Weight Using the Flow Polymerization Process

Water Content (ppm)	Temperature (°C)	M_w (Protected) kDa
50	−30	29.5
100	−30	17.3
200	−30	7.8
5	−20	24.3
50	−20	18
100	−20	12.1
5	−10	19.4
50	−10	13.4
200	−10	6.1

All polymerizations were performed using a 15:4:1 molar ratio of PiEVE:BVE:ODVE with a total monomer concentration of 0.45 M.

TABLE 2 Demonstration of the Relationship of Water Content and Temperature to Polymer Molecular Weight Using the Batch Polymerization Process

Water Content (ppm)	Temperature (°C)	M_w (Protected) kDa
10	−40	18
10	−35	16
35	−35	10
60	−12	8

All polymerizations were performed using a 15:4:1 molar ratio of PiEVE:BVE:ODVE.

variable, conjugates were prepared using polymers of the same molecular weight (M_w = 18 kDa (protected)/M_w = 9 kDa (deprotected), and using the same polymer:siRNA weight ratio. Two RNA sequences were selected, ZimmApoB which causes KD of ApolipoproteinB (ApoB), and a control sequence Low Hex 9 (LH9), which does not result in KD of any gene. Comparison of ApoB KD versus a control sequence assures that KD is specific and not a result of toxicity of the polymeric delivery vehicle. An identical process for generating polymer–siRNA conjugates was utilized for polymers made through both the flow and modified batch processes. Polymer-siRNA conjugates (**1a–c′** and **2a–c′**) were characterized to determine the siRNA conjugation efficiency (molar

percentage of total siRNA covalently attached to the polymer, Table 3) and the CDM masking efficiency (percentage of total amines in the polymer covalently modified with a CDM, Table 3).

Polymer-siRNA conjugation efficiency was high (>85%) and consistent across all polymer conjugates. CDM masking efficiency was consistent across all samples (50–62%). CD1 mice were dosed i.v. with a solution of polymer conjugates **1a–c′** and **2a–c′** via tail vein injection. Livers were harvested 48-h postdose and assayed for apoB mRNA levels relative to the mRNA levels of housekeeping genes PPIB and GAPDH using RT-qPCR.

Robust mRNA KD was observed for all ApoB containing polymer conjugates (**1a–b′** and **2a–b′**, Fig. 3); whereas, very low levels of KD were observed with the corresponding LH9 negative controls (**1c′** and **2c′**). However, polymer conjugates prepared from polymers made using the flow process (**1a′−b′**) were significantly more efficacious (95% KD) than polymer conjugates prepared from polymers made using the modified batch process (**2a′−b′**, 50% KD) at the same dose
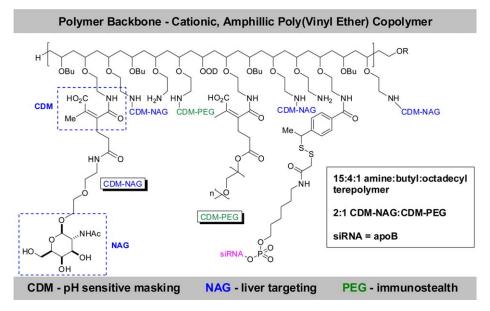

FIGURE 2 Graphical representation of dynamic polymer conjugate **1′**. [Color figure can be viewed in the online issue, which is available at wileyonlinelibrary.com.]

TABLE 3 Conjugation and Masking Efficiency Data for Polymer Conjugates Derived from Polymers Synthesized Using the Batch or Flow Polymerization Processes

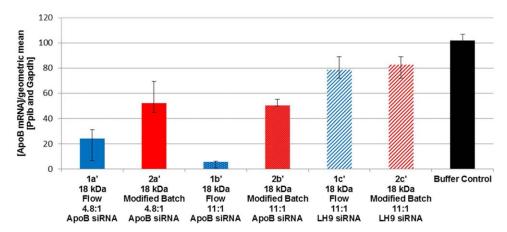| Polymer Conjugate	Method of Synthesis	M_w (Protected) kDa	PDI	RNA Sequence	Polymer:RNA wt:wt Ratio	Conjugation Efficiency (%)	Masking Efficiency (%)
1a′	Flow	18.1	1.7	ApoB	4.8:1	87	62
1b′	Flow	18.1	1.7	ApoB	11:1	91	51
1c′	Flow	18.1	1.7	LH9	11:1	85	55
2a′	Batch	18.3	1.8	ApoB	4.8:1	89	50
2b′	Batch	18.3	1.8	ApoB	11:1	92	55
2c′	Batch	18.3	1.8	LH9	11:1	90	53

FIGURE 3 Liver ApoB mRNA expression (mouse) at 3 mg/kg (48 h). [Color figure can be viewed in the online issue, which is available at wileyonlinelibrary.com.]

(3 mpk) and polymer:siRNA ratio (11:1). This difference in *in vivo* efficacy is suggestive that the method of synthesis of PVE polymers affects the structure of the resulting polymer, which in turn affects the *in vivo* properties of the resulting polyconjugate.

From the *in vivo* results, it is clear that PVE copolymers with the same M_w and overall monomer composition yield polymer conjugates that have dramatically different *in vivo* performance. In order to produce the desired cationic,
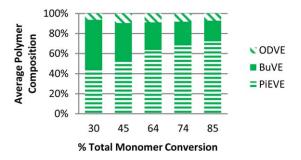
amphiphilic terpolymers, it is necessary to use a mixture of three vinyl ether monomers. From the literature, it is known that steric and electronic factors can often affect vinyl ether monomer reactivity and monomer reactivity will have a direct impact on polymer structure in a copolymerization.
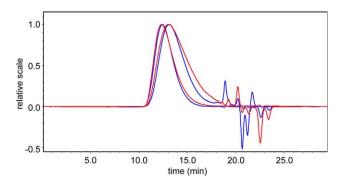

FIGURE 4 Plot showing average polymer composition versus total monomer conversion for a flow polymerization with an initial monomer charge of 15:4:1 PiEVE:BuVE:ODVE. [Color figure can be viewed in the online issue, which is available at wileyonlinelibrary.com.]

FIGURE 5 Size exclusion chromatographs for 18 kDa polymer synthesized using either the flow polymerization (M_w = 18.3 kDa, PDI 1.6) or batch addition processes (M_w = 18.2 kDa, PDI 1.7). The solid lines are refractive index traces, red for flow polymer; blue for batch addition polymer. The dotted lines are MALS (multiangle light scattering) traces, red for flow polymer and blue for batch addition polymer. [Color figure can be viewed in the online issue, which is available at wileyonlinelibrary.com.]

TABLE 4 Conjugation and Masking Efficiency Data for Polymer Conjugates Derived from Polymers Synthesized Using the Flow Polymerization Process

Polymer Conjugate	Method of Synthesis	M_w (Protected) kDa	PDI	RNA Sequence	Polymer:RNA wt:wt Ratio	Conjugation Efficiency (%)	Masking Efficiency (%)
1a′	Flow	18.1	1.7	ApoB	4.8:1	87	62
3a′	Flow	27.1	2.2	ApoB	4.8:1	92	50
3b′	Flow	29.4	2.0	ApoB	4.8:1	85	55
3c′	Flow	28.0	2.8	ApoB	4.8:1	89	53

The composition of a copolymer cannot be determined from knowledge of the homopolymerization rates of the monomers, as the relative rates of monomer copolymerization often bear little resemblance to the relative rates of homopolymerization.[33,34] In order to understand monomer reactivity in the terpolymerization, the copolymerization must be quenched at various levels of monomer conversion. In the modified batch polymerization process, the reaction was so rapid that it was not possible to quench the reaction quickly enough to get a range of different levels of monomer consumption. However, manipulating reaction time in the flow polymerization process was quite straightforward and could be readily controlled by manipulation of the reaction residence time by varying the length of tubing between the initial mixing tee and the quenching mixing tee. In this way, it was possible to get a snapshot of the unconsumed monomer ratio at various levels of monomer conversion. From a series of quenching experiments, it was determined that phthalimide ethyl vinyl ether (PiEVE) is less reactive than the alkyl vinyl ethers (BVE, ODVE, Fig. 4). This differential reactivity leads to an average polymer composition that changes over time. The relative amount of PiEVE in the terpolymer at low conversion is lower than that contained at higher levels of conversion. Given the monomer reactivity data and difference in experimental setup, we anticipate that polymers produced by different methods may have a different distribution of monomers along the polymer chain. In the flow polymerization process, the catalyst and bulk monomer are introduced to each other simultaneously. In the batch polymerization process, monomer is being continuously added to a system that already contains growing polymer chains.
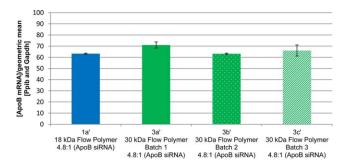
Given the nonliving nature of the polymerization, it is impossible to unambiguously define the polymer structure (Fig. 5). However, we speculate that polymers produced by a flow polymerization process have a more gradient-type structure while polymers produced by a modified batch process have monomers distributed more evenly throughout the polymer chain.

Flow Polymerization: Batch-to-Batch Comparison

Superior gene silencing was observed for polymer–siRNA conjugates made with polymers synthesized using the flow polymerization process. In order to demonstrate that the flow process was not only capable of producing polymer–siRNA conjugates that effect robust gene silencing but also of producing polymer–siRNA conjugates that reproducibly have the same biological activity as measured by *in vivo* mRNA KD, multiple batches of polymer were produced using the flow process. After deprotection, each polymer was conjugated to ApoB siRNA using an identical conjugation process. The masking efficiencies and siRNA conjugation efficiencies were consistent across all three polymer conjugates (Table 4). CD1 mice were dosed i.v. at 1 mpk with a solution of polymer conjugates **3a–c′** via tail vein injection.

FIGURE 6 Liver ApoB mRNA expression (mouse) at 1 mg/kg (48 h). [Color figure can be viewed in the online issue, which is available at wileyonlinelibrary.com.]
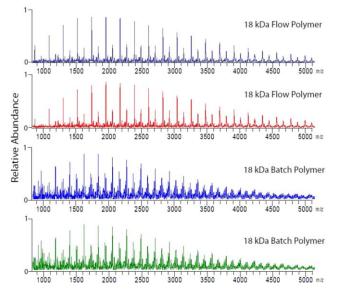

FIGURE 7 MALDI-TOF comparing protected polymers of the same average molecular weight (18 kDa) generated using the flow. [Color figure can be viewed in the online issue, which is available at wileyonlinelibrary.com.]

Livers were harvested 48-h postdose and assayed for apoB mRNA levels relative to the mRNA levels of housekeeping genes PPIB and GAPDH using RT-qPCR. Consistent mRNA KD was observed throughout the three batches of flow-based polymer conjugates (**1d–f'**; 29–37% KD, Fig. 6).

Analytical Comparison of Flow versus Batch Processes

In order to further illuminate structural differences in the polymers produced by these two processes, we analyzed the polymers by MALDI-TOF comparing protected polymers of the same average molecular weight (18 kDa) generated using the flow polymerization process and the batch polymerization process (Fig. 5). Polymer (1–5 mg/mL) in THF was mixed with the matrix solution (10 mg/mL sinapinic acid in THF) at a 1:1 ratio. The resulting mixtures were then deposited on the MALDI target. Each sample was analyzed twice to show the reproducibility of the analysis process. A Bruker Autoflex III mass spectrometer was used to analyze the samples in the positive, lineal mode. The resulting MS data (Fig. 7) were smoothed (SavtizkyGolay, 0.2 m/z width, one cycle) and baseline substracted (tophat algorithm). As shown in Figure 7, different "signatures" were observed for these two different polymer samples. Indeed, within this region, the major series of the MALDI signals have a difference of 100 Da, a likely indication of the incorporation of an extra BVE unit. This data is consistent with the method of synthesis affecting the composition of the copolymer.

CONCLUSIONS

We have developed two scaleable and reproducible processes to prepare terpolymers through a nonliving BF_3OEt_2-catalyzed polymerization. In addition to traditional analytical characterization, the polymer–siRNA conjugates derived from polymers produced using these two methods were characterized *in vivo*. Polymers made through the flow polymerization process were shown to be more efficacious when formulated as siRNA–polymer conjugates than those made through the modified batch process. This work illustrates that control over the method of polymer synthesis can affect the polymer produced, thus affecting the *in vivo* performance.

ACKNOWLEDGMENTS

REFERENCES AND NOTES

1 K. Gardikis, M. Micha-Screttas, C. Demetzos, B. R. Steele, *Curr. Med. Chem.* **2012**, *19*, 4913–4928.

2 S. R. Qureshi, Y. P. Sahni, S. K. Singh, M. A. Bhat, A. A. Dar, S. A. Quadri, Application of nanotechnology in cancer treatment. *J. Pharm. Res. Opin.* **2011**, *1*, 37–41.

3 N. Kamaly, Z. Xiao, P. M. Valencia, A. F. Radovic-Moreno, O. C. Farokhzad, *Chem. Soc. Rev.* **2012**, *41*, 2971–3010.

4 S. A. Unterman, N. A. Marcus, J. H. Elisseeff, Biodegrad. Polym. Clin. Use Clin. Dev. **2011**, 631–664.

5 T. Challa, B. A. Goud, S. Baskar, G. C. Mouli, R. Jukuri, *Int. J. Pharm. Sci. Rev. Res.* **2011**, *9*, 88–99.

6 P. Kumari, A. Tiwari, M. Prabaharan, S. Li, *Smart Polym. Mater. Biomed. Appl.* **2010**, 103–118.

7 M. Wang, M. Thanou, *Pharmacol. Res.* **2010**, *62*, 90–99.

8 M. Belting, A. Wittrup, *Mol. Biotechnol.* **2009**, *43*, 89–94.

9 D. B. Rozema, D. L. Lewis, D. H. Wakefield, S. C. Wong, J. J. Klein, P. L. Roesch, S. L. Bertin, T. W. Reppen, Q. Chu, A. V. Blokhin, J. E. Hagstrom, J. A. Wolff, *Proc. Natl. Acad. Sci.* **2007**, *104*, 12982–12987.

10 R. Gaspar, r.; R. Duncan, *Adv. Drug Delivery Rev.* **2009**, *61*, 1220–1231.

11 E. Wagner, *Adv. Polym. Sci.* **2012**, *247*, 1–29.

12 K. A. Whitehead, R. Langer, D. G. Anderson, *Nat. Rev. Drug Discov.* **2009**, *8*, 129–138.

13 M. G. Stanton, S. L. Colletti, *J. Med. Chem.* **2010**, *53*, 7887–7901.

14 C. Alabi, A. Vegas, D. Anderson, *Curr. Opin. Pharmacol.* **2012**, *12*, 427–433.

15 P. Vader, L. J. van der Aa, G. Storm, R. M. Schiffelers, J. F. J. Engbersen, *Curr. Top. Med. Chem.* **2012**, *12*, 108–119.

16 L. Sepp-Lorenzino, M. K. Ruddy, *Clin. Pharmacol. Ther.* **2008**, *84*, 628–632.

17 K. Singha, R. Namgung, W. J. Kim, *Nucleic Acid Ther.* **2011**, *21*, 133–147.

18 D. Fischer, Y. Li, *Biomaterials* **2003**, *24*, 1121–1131.

19 M. Morille, C. Passirani, A. Vonarbourg, A. Clavreul, J.-P. Benoit, *Biomaterials* **2008**, *29*, 3477–3496.

20 A. Kichler, *J. Gene Med* **2004**, *6*, S3–S10.

21 R. Kircheis, L. Wightman, E. Wagner, *Adv. Drug Delivery Rev.* **2001**, *53*, 341–358.

22 R. G. Parmar, M. Busuek, E. S. Walsh, K. R. Leander, B. J. Howell, L. Sepp-Lorenzino, E. Kemp, L. S. Crocker, A. Leone, C. J. Kochansky; B. A. Carr, R. M. Garbaccio, S. L. Colletti, W. W. Wang, *Bioconjugate Chem.* **2013**, *24*, 640–647.

23 S. E. Barrett, R. M. Garbaccio, R. A. Kowtoniuk, W. Wang, J. M. Williams, J. Liao, T. Pei, S. C. Tobias, **2013**, *PCT Int. Appl.* WO 2013016057 A1 20130131.

24 M. Busuek, R. G. Parmar, M. S. Poslusney, W. Wang, J. M. Williams, **2012**, *PCT Int. Appl.* WO 2012082574 A1 20120621.

25 S. E. Barrett, M. Busuek, S. L. Colletti, R. M. Garbaccio, E. N. Guidry, R. A. Kowtoniuk, J. Liao, C. A. Parish, R. G. Parmar, T. Pei, K. M. Schlosser, D. M. Tellers, S. C. Tobias, Q. T. Truong, J. H. Waldman, W. Wang, J. M. Williams, **2012**, *PCT Int. Appl.* WO 2012068187 A1 20120524.

26 M. Busuek, S. L. Colletti, R. G. Parmar, W. Wang, J. M. Williams, **2011**, *PCT Int. Appl.* WO 2011115862 A1 20110922.

27 C. Dohmen, E. Wagner, *Methods Mol. Bio.* **2011**, *683*, 453–463.

28 S. C. Wong, J. J. Klein, H. L. Hamilton, Q. Chu, C. L. Frey, V. S. Trubetskoy, J. Hegge, D. Wakefield, D. B. Rozema, D. Lewis, L Nucleic Acid Ther.**2012**, *22*, 380–390.

29 D. B. Rozema, K. Ekena, D. L. Lewis, A. G. Loomis, J. A. Wolff, *Bioconjugate Chem.* **2003**, *14*, 51–57.

30 M. Meyer, A. Zintchenko, M. Orgris, E. Wagner, *J. Gene Med* **2007**, *9*, 797–805.

31 M. Meyer, C. Dohmen, A. Philipp, D. Kiener, G. Maiwald, C. Scheu, M. Ogris, E. Wagner, *Mol. Pharm.* **2009**, *6*, 752–762.

32 M. Meyer, A. Philipp, R. Oskuee, C. Schmidt, E. Wagner, *J. Am. Chem. Soc.* **2008**, *130*, 3272-32–73.

33 G. Odian, Principles of Polymerization; Wiley: New York, **1991**; 356–398.

34 K. Matyjaszewski, Cationic Polymerizations: Mechanisms, Synthesis and Applications; Marcel Dekker: New York, **1996**.

35 J.-i. Yoshida, Flash Chemistry: Fast Organic Synthesis in Microsystems; Wiley: UK, **2008**.

36 C. Tonhauser, A. Natalello, H. Lowe, H. Frey, *Macromolecules* **2012**, *45*, 9551–9570.

37 L. F. Raveglia, G. A. M. Giardina, *Future Med. Chem.* **2009**, *1*, 1019–1023.

38 T. S. Zimmermann, A. C. H. Lee, A. Akinc, B. Bramlage, D. Burncrot, M. N. Fedoruk, J. Harborth, J. A. Heyes, L. B. Jeffs, M. John, A. D. Judge, K. Lam, K. McClintock, L. V. Nechev, L. R. Palmer, T. Racie, I. Rohl, S. Seiffert, S. Shanmugam, V. Sood, J. Soutschek, I. Toudjarska, A. J. Wheat, E. Yaworski, W. Zedalis, V. Koteliansky, M. Manoharan, H.-P. Vornlocher, I. MacLachlan, *Nature* **2006**, *441*, 111–114.